

Regular article

An adaptive Rothe method for the wave equation

Martin Schemann¹, Folkmar A. Bornemann^{2*}

¹ Konrad-Zuse-Zentrum, Takustr. 7, D-14195 Berlin, Germany (e-mail: schemann@zib.de)

² Courant Institute of Mathematical Sciences, 251 Mercer St, New York NY 10012, USA (e-mail: bornemann@na-net.ornl.gov)

Accepted: 12 August 1997

Communicated by P. Deuffhard

Abstract. The adaptive Rothe method approaches a time-dependent PDE as an ODE in function space. This ODE is solved *virtually* using an adaptive state-of-the-art integrator. The *actual* realization of each time-step requires the numerical solution of an elliptic boundary value problem, thus *perturbing* the virtual function space method. The admissible size of that perturbation can be computed *a priori* and is prescribed as a tolerance to an adaptive multilevel finite element code, which provides each time-step with an individually adapted spatial mesh. In this way, the method avoids the well-known difficulties of the method of lines in higher space dimensions. During the last few years the adaptive Rothe method has been applied successfully to various problems with infinite speed of propagation of information. The present study concerns the adaptive Rothe method for hyperbolic equations in the model situation of the wave equation. All steps of the construction are given in detail and a numerical example (diffraction at a corner) is provided for the 2D wave equation. This example clearly indicates that the adaptive Rothe method is appropriate for problems which can generally benefit from mesh adaptation. This should be even more pronounced in the 3D case because of the strong Huygens' principle.

Introduction

Adaptive methods become particularly important for the efficient and reliable numerical solution of time dependent PDEs in the presence of transient phases and sharply localized phenomena. There are two principal choices if one wishes to avoid a nonuniform subdivision of the whole space-time domain, and stays with a time-marching approach:

- Discretization in space first, known as the “method of lines.” This creates an ordinary differential equation which can be solved by a state-of-the-art numerical integrator. However, the spatial mesh-points stay fixed in time, or in the case of a moving mesh, are often subject to severe restraints. Thus, the method has considerable difficulties in

changing the spatial mesh appropriately in higher dimensions.

- Discretization in time first, known as the “Rothe method.” Here, one first applies an adaptive time-marching scheme to an appropriate reformulation of the problem as an ODE in function space. Each time-step results in an elliptic boundary value problem, which can be solved effectively by an adaptive finite element method. By this means, an appropriate spatial mesh is introduced for each individual time-step.

The advantages of the latter approach were shown by the second author in a series of papers [2–4] for linear *parabolic equations*. It was demonstrated that an adaptive finite element code such as KASKADE [1, 15] could be applied successfully as a *black box*. Only a *tolerance* has to be prescribed for the elliptic solver at each time-step. This single number is chosen such that a more accurate solution of the elliptic problem would not change the time-step—at least not locally. This general method was called *adaptive Rothe method* and numerical experiments have confirmed its efficiency.

This approach was later extended to several equations of importance in applications—including problems not of parabolic type, e.g.,

- the so-called bio-heat-transfer-equation [4]
- Schrödinger's equation and Fresnel's wave equation¹ [25, 26]
- nonlinear reaction-diffusion equations [14, 22]
- nonlinear ODEs in infinite dimensional sequence spaces, as arising in polymer chemistry and statistics [28]

All these equations have *infinite speed* of propagation of information. This makes the adaptive Rothe method particularly well suited since there is a clear cut distinction between time and space.

Hyperbolic equations have a different character: there are finite speeds of propagation, which blurs the distinction between time and space; the “light-cone” only provides a distinction between “time-like” and “space-like” directions. The

* The work of this author was supported in part by the U.S. Department of Energy under contract DE-FG02-92ER25127.

¹ Note, that Fresnel's equation is parabolic in the damped case and of Schrödinger type in the loss-free case.

aim of this paper is to study the adaptive Rothe method in detail in a hyperbolic model case. The principal design steps of the method and the necessary tolerance formulas for controlling the black box elliptic solver are presented. A numerical example—so far for the 2D case only—clearly indicates, that the adaptive Rothe method is appropriate for problems which can benefit from mesh adaptation in general.

Our paper is organized as follows:

In Section 1, we reformulate the wave equation as an ODE with an infinite-dimensional state space, i.e., as an abstract Cauchy problem in a certain Hilbert space.

In Section 2, we discuss single-step methods which can be applied to this abstract Cauchy problem and their approximation and conservation properties.

In Section 3, we introduce the adaptive time-step algorithm in Hilbert space. Note, that this algorithm is *virtual*: in reality there are perturbations by a discretization in space.

In Section 4, we derive the tolerances which have to be prescribed to the discretization in space. They are chosen such that the time-step is not changed noticeably and that a user given tolerance in time is matched.

In Section 5, we finally show how the design principles are reflected in the actual performance of the method in 2D. We have chosen a diffraction problem, where adaptivity pays off in the beginning because of the large “shadow regions.” We also indicate why adaptivity will be even more important in the 3D case, where in contrast to the 2D case the strong Huygens’ principle predicts growing “shadow regions” whenever sharply localized initial data are given.

1 The continuous problem

For the sake of simplicity we restrict ourselves to the *homogeneous wave equation*

$$y_{tt}(t, x) - c^2 \Delta y(t, x) = 0, \quad x \in \Omega, \quad t \in]0, T]$$

with wave speed $c > 0$, homogeneous Dirichlet boundary conditions

$$y(t, \cdot)|_{\partial\Omega} = 0, \quad t \in]0, T],$$

and initial data²

$$y(0, \cdot) = y_0 \in H_0^1(\Omega), \quad y_t(0, \cdot) = z_0 \in L^2(\Omega).$$

Here, $\Omega \subset \mathbb{R}^d$ denotes a bounded Lipschitz domain and $T > 0$ a fixed final time. We will apply semi-group theory as the tool for establishing existence and uniqueness and—even more important—error estimates of semi-discretizations in time. To this end, we have to reformulate our problem accordingly.

Let L denote the selfadjoint Friedrichs representation operator $L : D_L \subset L^2(\Omega) \rightarrow L^2(\Omega)$ of the Dirichlet form $(\nabla u, \nabla v)_{L^2}$, i.e.,

$$(Lu, v)_{L^2} = (\nabla u, \nabla v)_{L^2} \quad u \in D_L, \quad v \in H_0^1(\Omega),$$

² All function spaces are understood to comprise *complex-valued* functions.

cf. [21, pp. 332ff]. For $s \geq 0$, we introduce the smoothness spaces $H^{2s} = D_{L^s}$. Using the Poincaré-Friedrichs inequality, we can equip the Hilbert space

$$H = H_0^1(\Omega) \times L^2(\Omega)$$

with the energy inner product of our problem, i.e.,

$$a(u, v) = c^2(\nabla u_1, \nabla v_1)_{L^2} + (u_2, v_2)_{L^2}, \\ u = (u_1, u_2), \quad v = (v_1, v_2) \in H.$$

The corresponding *energy norm* of H is denoted as

$$\|u\|_a^2 = a(u, u) \quad u \in H.$$

Deploying the unbounded, densely defined, and closed operator

$$A : D_A = \dot{H}^2 \times H_0^1(\Omega) \subset H \rightarrow H,$$

where

$$Au = (u_2, -c^2 Lu_1) \quad u = (u_1, u_2) \in D_A,$$

yields an equivalent formulation of the wave equation as the following abstract, first order Cauchy problem

$$u_t = Au, \quad u(0) = u_0 \in H,$$

with the solution and initial data

$$u = (y, y_t), \quad u_0 = (y_0, z_0).$$

Lemma 1 *The operator A , defined as above, is skew-adjoint with respect to the energy inner product on H .*

Proof. Let $u = (u_1, u_2), v = (v_1, v_2) \in D_A$ be given. The skew-symmetry of A is best visible in the second row of the following formula

$$a(Au, v) = c^2(\nabla u_2, \nabla v_1)_{L^2} - c^2(Lu_1, v_2)_{L^2} \\ = c^2((Lu_2, v_1)_{L^2} - (u_1, Lv_2)_{L^2}) \\ = -a(u, Av)$$

and implies that $-A^*$ is an extension of A as a densely defined closed operator. By the maximality of the Friedrichs representation L , we conclude that in fact $A = -A^*$. \square

Corollary 2 *The operator A generates a C_0 -group $\exp(tA)$ of operators which are unitary with respect to the energy norm of H . In particular, the solution of the abstract Cauchy problem is uniquely given by*

$$u(t) = \exp(tA)u_0 \in H.$$

It conserves the smoothness norm

$$\|A^s u(t)\|_a = \|A^s u_0\|_a, \quad t \in \mathbb{R}, \quad (1)$$

for $u_0 \in D_{A^s}$ and $s \in \mathbb{N}_0$. Hence, D_{A^s} is an invariant subspace under the action of the group.

Proof. The operator A/i is selfadjoint and Stone’s theorem [23] implies that A is generating a C_0 -group $\exp(tA) = \exp(itA/i)$ of *unitary* operators on H . The norm conservation follows from the fact that A commutes with the group. \square

The special case $s = 0$ of formula (1) is just an abstract reformulation of the well known conservation of energy of the wave equation [20, p. 139].

2 Semi-discretization in time

We consider single-step methods which are given by a rational approximation R of the exponential function with *consistency* order $p \in \mathbb{N}$,

$$|R(z) - \exp(z)| = O(|z|^{p+1}), \quad z \rightarrow 0.$$

We assume throughout that the rational function is A -stable³, i.e.,

$$\Re z \leq 0 \Rightarrow |R(z)| \leq 1.$$

The single-step method approximating the abstract Cauchy problem is now given by the time-marching scheme

$$u_{n+1} = R(\tau A)u_n,$$

where τ denotes the time-step. In a seminal paper, Brenner and Thomée have shown [11, Theorem 4] that the following error estimate holds.

Theorem 3 *Let R be an A -stable rational approximation of order p of the exponential function. Then, the estimate*

$$\|u_n - u(t)\|_a \leq Ct^{s-\beta(s)}\tau^{\beta(s)}\|A^s u_0\|_a, \quad u \in D_{A^s} \quad (2)$$

holds uniformly for $t = n\tau$, where $\beta(s) = sp/(p+1)$ and $s \in \mathbb{N}$ is restricted to $(p+1)/2 < s \leq p+1$.

Later on we will use the implicit Euler scheme

$$R_E(z) = \frac{1}{1-z},$$

which is of order $p = 1$, yielding the single-step solution u_n^E , and the Crank-Nicolson scheme

$$R_{CN}(z) = \frac{1+z/2}{1-z/2},$$

which is of order $p = 2$, yielding the single-step solution u_n^{CN} .

Lemma 4 *If the regularity of the initial data $u_0 = (y_0, z_0)$ of the wave equation is given by $y_0 \in \dot{H}^2$ and $z_0 \in \dot{H}^2$, then the error estimates*

$$\|u_n^E - u(t)\|_a \leq Ct\tau, \quad \|u_n^{CN} - u(t)\|_a \leq Ct^{2/3}\tau^{4/3},$$

hold for all $t = n\tau$. Imposing the higher regularity $y_0 \in \dot{H}^4$ and $z_0 \in \dot{H}^2$ yields the error estimates

$$\|u_n^E - u(t)\|_a \leq Ct\tau, \quad \|u_n^{CN} - u(t)\|_a \leq Ct\tau^2,$$

for all $t = n\tau$.

³ Since the spectrum of a skew-adjoint operator is purely imaginary, A -stability might appear unnecessarily restrictive. One would rather expect the assumption of I -stability, i.e., $|R(ix)| \leq 1$ for all $x \in \mathbb{R}$. However, it was shown in [27] that a j -stage I -stable Runge-Kutta method of order $p \geq 2j - 1$ is A -stable. Thus, there is no restriction for all practical reasons. Furthermore, no generalization of Theorem 3 is known for I -stable methods which are not A -stable.

Proof. We note that

$$A^2 u_0 = -c^2(Ly_0, Lz_0), \quad A^3 u_0 = -c^2(Lz_0, -c^2 L^2 y_0), \\ u_0 = (y_0, z_0),$$

and therefore

$$u_0 \in D_{A^2} \Leftrightarrow y_0 \in \dot{H}^2, z_0 \in \dot{H}^2, \\ u_0 \in D_{A^3} \Leftrightarrow y_0 \in \dot{H}^4, z_0 \in \dot{H}^2.$$

We can now use Theorem 3. \square

Since the norm conservation (1), in particular for $s = 0$, is an important feature of the continuous model it is natural to consider single-step methods which are energy conserving, i.e., for which $R(\tau A)$ is a *unitary* operator with respect to the energy norm. A useful criterion is provided by the following Lemma.

Lemma 5 *If a rational approximation R of the exponential function with real coefficients fulfills*

$$R(z)R(-z) = 1 \quad \forall z \in \mathbb{C}$$

and has no poles in the left half-plane, then R is an A -stable approximation of the exponential function and $R(\tau A)$ is unitary with respect to the energy inner product, i.e.,

$$R(\tau A)R(\tau A)^* = I.$$

Proof. Applying any operational calculus for unbounded operators, e.g., the Dunford-Taylor calculus [16], and using the skew-adjointness $A^* = -A$ yields

$$I = R(\tau A)R(-\tau A) = R(\tau A)R(\tau A^*)$$

as a consequence of $R(z)R(-z) = 1$. It remains to show that $R(\tau A^*) = R(\tau A)^*$. This, surprisingly, requires some work.

Using that $R(z)R(-z) = 1$ and the maximum principle one can show the A -stability of R , cf. [13, Lemma 6.20]. Hence, by a result of Brenner and Thomée [11, p. 685], there exists a bounded measure μ on \mathbb{R}_+ such that R is the Laplace-Stieltjes transform of μ ,

$$R(z) = \int_0^\infty e^{z\lambda} d\mu(\lambda), \quad \Re z \leq 0.$$

Now, the fact that R has real coefficients immediately implies that μ is *real-valued*. Applying the Hille-Phillips functional calculus [19], we get

$$R(\tau A^*) = \int_0^\infty \exp(\tau\lambda A^*) d\mu(\lambda) = \int_0^\infty \exp(\tau\lambda A)^* d\mu(\lambda) \\ = \left(\int_0^\infty \exp(\tau\lambda A) d\mu(\lambda) \right)^* = R(\tau A)^*.$$

The second equality follows from Stone's theorem and the third equality holds since μ is real-valued. Note, that all integrals represent bounded linear operators on H . \square

The Crank-Nicolson scheme satisfies the assumption of Lemma 5 which implies the well-known conservation of energy of the corresponding semi-discretization in time. Note, that $R_{\text{CN}}(\tau A)$ being unitary also follows from observing that $-R_{\text{CN}}(\tau A)$ is the Cayley transform of the selfadjoint operator $\tau A/2i$, cf. [24, Theorem 13.19].

Corollary 6 *Let $u_0 \in D_{A^s}$, $s \in \mathbb{N}_0$ be given. The semi-discretization in time given by the Crank-Nicolson scheme conserves the corresponding smoothness norm,*

$$\|A^s u_n^{\text{CN}}\|_a = \|A^s u_0\|_a, \quad n = 1, 2, \dots$$

In particular, D_{A^s} is an invariant subspace under the action of the Crank-Nicolson scheme.

Proof. The fact that the operator $R_{\text{CN}}(\tau A)$ is unitary proves the case $s = 0$. The other cases follow from the commutativity $AR(\tau A) = R(\tau A)A$. \square

Note, that this result immediately extends to all implicit Runge-Kutta methods based on Gauss-Legendre quadrature [13, 18].

3 The Hilbert space algorithm

The backbone of the adaptive Rothe method is the application of ODE-techniques [13, 17, 18] to the abstract Cauchy problem. Modern integrators for ODEs adapt the time-step in such a way that it is as large as possible while the local error estimate matches a user prescribed tolerance TOL. To this end, a simple feedback control loop is used which can be described by just explaining the first step of a single-step method.

For a given initial value $u_0 \in D_{A^2}$, and a step size guess τ_0 , two approximations of *different* accuracy are computed, e.g.,

$$u_1^{\text{E}} = R_{\text{E}}(\tau_0 A)u_0, \quad u_1^{\text{CN}} = R_{\text{CN}}(\tau_0 A)u_0.$$

If τ_0 is small enough, we may assume by referring to Lemma 4 that

$$\epsilon = \|u_1^{\text{E}} - u_1^{\text{CN}}\|_a \approx \|u_1^{\text{E}} - \exp(\tau_0 A)u_0\|_a.$$

A reasonable new time-step τ_{new} , which tries to push the error ϵ near to but below TOL, would thus be given by

$$\tau_{\text{new}} = \sigma \sqrt{\frac{\text{TOL}}{\epsilon}} \tau_0,$$

where $\sigma < 1$ is a safety factor. Note, that this formula takes the asymptotic behavior of the implicit Euler method for $\tau \rightarrow 0$ into account. However, using arguments from *control theory* one can show, that this proposal is a robust device even if the asymptotics is seriously perturbed, cf. [13]. Now, we distinguish two cases:

- $\epsilon > \text{TOL}$. We repeat the step with the same u_0 , but replace the time-step τ_0 by τ_{new} .
- $\epsilon \leq \text{TOL}$. We set $u_1 = u_1^{\text{CN}} \in D_{A^2}$ and $\tau_1 = \tau_{\text{new}}$ and progress as in the first step.

The choice $u_1 = u_1^{\text{CN}}$ is made for two reasons: First, u_1^{CN} is more accurate than u_1^{E} and second, it conserves energy which is crucial.

4 Perturbations by finite element solution

The actual approximation of the Crank-Nicolson and of the implicit Euler step using linear finite elements yields perturbations which we denote by

$$\hat{u}_1^{\text{CN}} = u_1^{\text{CN}} + \delta_{\text{CN}}, \quad \hat{u}_1^{\text{E}} = u_1^{\text{E}} + \delta_{\text{E}}.$$

The idea of the adaptive Rothe method, as introduced by Bornemann [3], is to control the perturbations δ_{CN} and δ_{E} by an adaptive finite element method in such a way that the time-step sequence is not influenced in an essential way. We set

$$\hat{\epsilon} = \|\hat{u}_1^{\text{CN}} - \hat{u}_1^{\text{E}}\|_a, \quad \Theta = \|\delta_{\text{CN}}\|_a + \|\delta_{\text{E}}\|_a,$$

and take the *computable* new time-step

$$\hat{\tau}_{\text{new}} = \sigma \sqrt{\frac{\text{TOL}}{\hat{\epsilon}}} \tau_0$$

instead of the *virtual* τ_{new} . Using the trivial estimate

$$\hat{\epsilon} - \Theta \leq \epsilon \leq \hat{\epsilon} + \Theta,$$

we notice that the constraint

$$\Theta \leq \hat{\epsilon}/4 \tag{3}$$

guarantees

$$0.89 \hat{\tau}_{\text{new}} \leq \tau_{\text{new}} \leq 1.16 \hat{\tau}_{\text{new}},$$

which seems to be a tolerable range in practice. We realize the condition (3) by using error estimators

$$\|\delta_{\text{CN}}\|_a \approx [\delta_{\text{CN}}], \quad \|\delta_{\text{E}}\|_a \approx [\delta_{\text{E}}].$$

Here and in what follows, we use square brackets for denoting an estimator of some error quantity. The final error control in each step is given by splitting the tolerance in an appropriate way,

$$\begin{aligned} [\delta_{\text{CN}}], [\delta_{\text{E}}] &\leq (1 - \rho) \text{TOL}/2, \\ 4(1 - \rho) \text{TOL} &\leq \hat{\epsilon} \leq \rho \text{TOL}. \end{aligned} \tag{4}$$

Note, that the first two are conditions on the finite element solution whereas the third is a condition on the time-step. We have to require $\rho \geq 0.8$ and in practice we use

$$\rho_* = 5/6 = 0.83333 \dots,$$

which means that the spatial problems have to be solved ten times as accurately as the time-marching loop: $(1 - \rho_*) \text{TOL}/2 = 0.1 \rho_* \text{TOL}$. This also helps to assure energy conservation since the finite element solution does *not exactly* conserve energy but keeps it nearly constant within the given range of accuracy.

Adaptive finite element codes such as KASKADE [15, 8] do usually not provide the error estimators $[\delta_{\text{CN}}]$ and $[\delta_{\text{E}}]$ directly. One has to relate them to the energy norm of the elliptic problem under consideration. This will be worked out next.

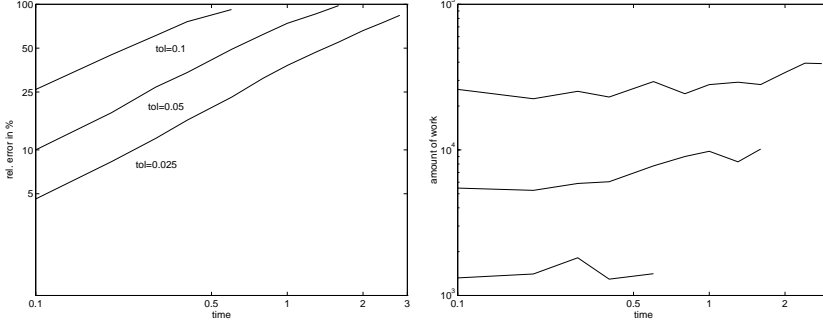


Fig. 1. *Left:* Relative error $\epsilon(t)$ vs. time for different tolerances TOL (Example 1). *Right:* Number of nodal points vs. time for different tolerances TOL (Example 1).

We analyze the Crank-Nicolson and the implicit Euler step and recall that there are two components $u = (y, z)$ since we have reformulated the wave equation as a first order system. Let $u_j = (y_j, z_j)$, $\hat{u}_j = (\hat{y}_j, \hat{z}_j)$, and $\delta = (\eta, \zeta)$. The superscripts CN and E will only be used when a distinction is necessary and not clear from the context.

The Crank-Nicolson step is given by

$$\left(I + \frac{\tau^2 c^2}{4} L\right) y_1 = \left(I - \frac{\tau^2 c^2}{4} L\right) y_0 + \tau z_0,$$

$$z_1 = \frac{2}{\tau}(y_1 - y_0) - z_0.$$

The first equation is solved by a finite element method and yields an approximation for which we control the error η in the energy norm of the elliptic operator $I + \tau^2 c^2 L/4$. Therefore, an adaptive finite element method provides the error estimator

$$[\eta]^2 \approx \|\eta\|_{L^2}^2 + \frac{\tau^2 c^2}{4} |\eta|_{H^1}^2.$$

The second equation yields \hat{z}_1 after a projection or interpolation of y_0 and z_0 . We may assume that the projection or interpolation errors are considerably smaller than $2[\eta]/\tau$ and obtain

$$\|\zeta\|_{L^2}^2 \approx \frac{4}{\tau^2} \|\eta\|_{L^2}^2.$$

Altogether, we get that

$$\|\delta\|_a^2 = c^2 |\eta|_{H^1}^2 + \|\zeta\|_{L^2}^2 \approx \frac{4}{\tau^2} [\eta]^2,$$

which makes it natural to define the error estimator

$$[\delta^{\text{CN}}] = \frac{2}{\tau} [\eta^{\text{CN}}].$$

Likewise, the implicit Euler step reads as

$$(I + \tau^2 c^2 L) y_1 = y_0 + \tau z_0,$$

$$z_1 = \frac{1}{\tau}(y_1 - y_0).$$

Arguing as above, we obtain the estimator

$$[\eta]^2 \approx \|\eta\|_{L^2}^2 + \tau^2 c^2 |\eta|_{H^1}^2, \quad \|\zeta\|_{L^2}^2 \approx \frac{1}{\tau^2} \|\eta\|_{L^2}^2$$

and get

$$\|\delta\|_a^2 = c^2 |\eta|_{H^1}^2 + \|\zeta\|_{L^2}^2 \approx \frac{1}{\tau^2} [\eta]^2.$$

Therefore, it is natural to define

$$[\delta^{\text{E}}] = \frac{1}{\tau} [\eta^{\text{E}}].$$

Hence, the error criterion (4) will be implemented in the form

$$[\eta^{\text{CN}}] \leq \tau(1 - \rho) \text{TOL} / 4, \quad [\eta^{\text{E}}] \leq \tau(1 - \rho) \text{TOL} / 2. \quad (5)$$

5 Numerical examples

The method introduced above has been implemented in the 2D case using the program KASKADE 3.0 as the black box solver of the elliptic problems. KASKADE 3.0 dates back to work of Deuffhard, Leinen, and Yserentant [15] and was later improved by Bornemann, Erdmann, and Kornhuber [7, 8]. Its present implementation at the Konrad-Zuse-Zentrum Berlin is due to Beck, Erdmann, and Roitzsch [1]. It features all the properties which are needed for the adaptive Rothe method and offers two fast multilevel solvers for elliptic problems of the type

$$(I + \tau^2 L)u = f.$$

Both have multigrid complexity $O(N)$, where N is the number of nodal points. This complexity bound holds *uniformly* in the time-step τ . One fast solver is a τ -dependent modification of the BPX method [10] developed by Bornemann [4]; the other is the cascadic multilevel method developed by Deuffhard [12] and studied by Bornemann, Deuffhard, and Krause [5, 6, 9]. The mass matrix is stabilized by lumping for very small time-steps.

5.1 Hyperbolic transport

We will discuss an essentially one-dimensional transport problem, which is suited to address such topics as stability and robustness of the adaptive strategy and accumulation of errors. With respect to the latter, one might expect a behavior of the adaptive Rothe method much less favorable as compared to parabolic problems because there is no damping in hyperbolic problems. However, we will show a performance which is decisively better than this expectation.

We consider the 2D homogeneous wave equation with wave speed $c = 1$ on the domain $\Omega =]0, 3[\times]0, 0.25[$, choosing initial data and boundary values such that the solution is given by the following transported Gaussian

$$y(t, x_1, x_2) = 0.1 \exp(-400 \cdot (0.125 + t - x_1)^2).$$

This way, we take homogeneous Neumann boundary conditions on the boundary pieces parallel to the x_1 -axis, and for $t \in [0, 2.75]$, as a good approximation within the accuracy range to be chosen, Dirichlet boundary conditions on those boundary pieces parallel to the x_2 -axis. We have performed runs for the tolerances $\text{TOL} = 0.1$, $\text{TOL} = 0.05$, and $\text{TOL} = 0.025$ until that time t at which a 100% relative error $\epsilon(t)$ was accumulated,

$$\epsilon(t) = \max_{s \in [0, t]} \frac{\|y_{\text{numerical}}(s) - y(s)\|_a}{\|y(s)\|_a}.$$

As shown in Fig. 1, in a double logarithmic plot of $\epsilon(t)$ vs. t we get equally spaced parallel lines,

$$\epsilon(t) \propto \text{TOL} \cdot t^\beta, \quad \beta \approx 0.9. \quad (6)$$

Here, the adaptive strategy realizes nearly constant time steps, independently of the actually accumulated error. Thus, since error in time is only controlled in keeping it *locally* constant, there is no influence of the tolerated *overall* errors on the performance of the adaptive strategy. Moreover, the observed near linear increase of the error in time is in perfect accordance with the theoretical result of Lemma 4.

Also, the deviation from energy conservation increases like Eq. (6). However, the constants are much smaller: for $\text{TOL} = 0.025$ there is a 0.3% deviation from energy conservation at $t = 0.1$ (13 time-steps, solution error 4.6%) and a 5.6% one at $t = 2.75$ (342 time-steps, solution error 83%).

The number of nodal points increases only slightly with time, mainly due to small high frequency errors introduced by the adaptive meshing in space. However, comparable in size to this increase there is a fluctuation which is caused by geometric effects of the triangulation, see Fig. 1.

Altogether, this example shows that the adaptive strategy is a stable and robust device which, first, is not affected by accumulation of errors in time, and second, accumulates errors in a predictable way—even for long term computations.

5.2 Diffraction at a corner

Given the L-shaped domain

$$\Omega = \{(x_1, x_2) : 0.5 < x_1 < 1 \text{ and } 0 < x_2 \leq 0.5\} \\ \cup \{(x_1, x_2) : 0 < x_1 < 1 \text{ and } 0.5 < x_2 < 1\}$$

with boundary segments $\Gamma_1 = \{x \in \partial\Omega : x_2 = 1\}$ and $\Gamma_2 = \partial\Omega \setminus \Gamma_1$, we consider the wave equation with wave speed $c = 1$, homogeneous Dirichlet boundary conditions on Γ_1 and homogeneous Neumann boundary conditions on Γ_2 . The initial values are

$$z_0 = 0, \\ y_0(x) = \begin{cases} -\omega \cdot \sin(2\pi k x_2 / S) & \text{for } x_2 \in [0, S], \\ 0 & \text{for } x_2 \in [S, 1]. \end{cases}$$

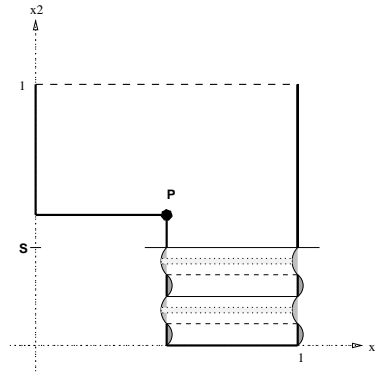


Fig. 2. Geometry of the initial data (Example 2)

Table 1. Performance data for Example 2

# step	time	θ_{time}	θ_{space}	$\ \hat{u}_n^{\text{CN}}\ _a$	τ	τ_{new}/τ	# nodal points
1	0.014	0.81	0.16	0.48	0.014	1.96	3876
15	0.194	0.74	0.15	0.47	0.013	1.00	11884
30	0.394	0.77	0.17	0.47	0.014	1.00	12166
45	0.593	0.74	0.15	0.46	0.013	1.01	22227

These initial data are depicted in Fig. 2. They resemble a monochromatic plane wave propagating in the x_2 direction which is diffracted at the point P into the shadow region of geometrical optics. Even though these initial data are slightly less regular as required by the theory above, the adaptive strategy leads to stable results, resembling the efficiency and asymptotic behavior of more regular data. We suggest that this can be understood by considering the adaptive algorithm as a stable feedback control device. Using such an argument, Bornemann and Deuffhard [13, pp. 178ff.] have been able to explain why step-size control for ordinary differential equations still works if there appears a sudden decrease of regularity.

The parameters of our example are given by

$$k = 2, \quad S = 0.4, \quad \omega = 0.05, \quad \text{TOL} = 0.15.$$

We computed 45 time-steps. Figs. 3 and 4 show the solution and triangulation for time-step # 20, # 30, and # 40.

Table 1 provides some relevant information every 15th step. Here, we define the ratios

$$\theta_{\text{space}} = \frac{4[\eta^{\text{CN}}]}{\tau \text{TOL}}, \quad \theta_{\text{time}} = \frac{\hat{\epsilon}}{\text{TOL}}.$$

Because of the error criteria (4) and (5) we have $4(1 - \rho_*) = 0.67 \dots \leq \theta_{\text{time}} \leq \rho_* = 0.83 \dots$ and $\theta_{\text{space}} \leq (1 - \rho_*) = 0.17 \dots$. Small values of θ_{time} and θ_{space} indicate that the method computes unnecessarily accurate solutions which means a loss in efficiency. Note, however, how close the computed values of θ_{time} and θ_{space} are to their upper bounds.

The time-step has been *automatically* chosen to be one tenth of a period of the monochromatic wave. This seems quite reasonable given the prescribed 15% accuracy. Note, that since the solution propagates into the shadow region the number of nodal points has to increase steadily with time. The observed 4% loss of energy is due to the fact that the triangulations are

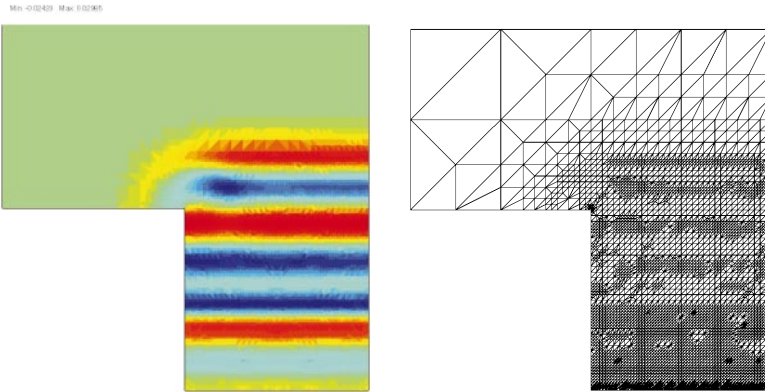


Fig. 3. Solution and triangulation for time-step # 20, $t = 0.27$, (Example 2). Notice that the upper boundary of the initial perturbation was located at $x_2 = 0.4$. The *color-coding* is chosen as follows: the green of the upper left corner belongs to zero, the maximum negative value is dark blue, the maximum positive value dark red. In between, the colors are distributed as in the spectrum of visible light.

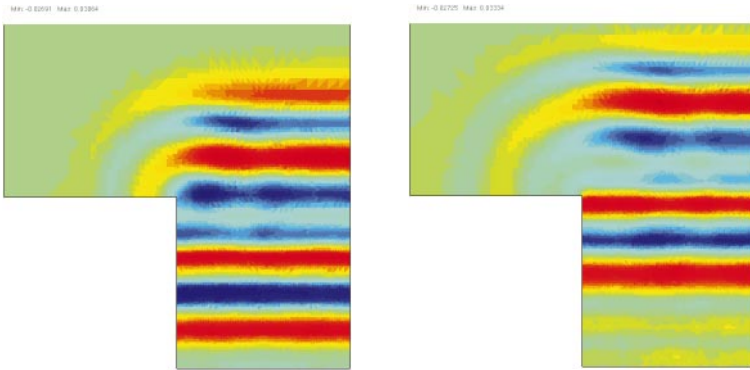


Fig. 4. Solution for time-step # 30, $t = 0.39$, and # 40, $t = 0.54$, (Example 2). Again, notice that the upper boundary of the initial perturbation was located at $x_2 = 0.4$. Color-coding as in Fig. 3.

changing at each time-step and the finite element projection does not exactly conserve energy. However, this error is well below the prescribed space error tolerance.

In the “lighted region” the algorithm chooses a nearly uniform mesh-size of $h \approx \tau/2$. At time-step 45 this region fills up the whole domain, which explains that the number of nodal points is roughly given by $N \approx 3h^{-2}/4 \approx 20000$. Thus, if one measures the work of the method by the number of degrees of freedom, it corresponds to the work of an explicit method with uniform time-space grid and a CFL-number of roughly 2.

As has to be expected, adaptivity offers no benefit at the end of the computation. However, during the earlier stages up to 6 times as many nodal points would be required using a uniform mesh. A 3D problem would benefit from adaptivity *at all times* because of the strong Huygens’ principle. We will return to that point in our conclusion.

6 Conclusion

We have shown that the adaptive Rothe method is a successful adaptive device for problems with finite propagation speed. It requires only a simple outer loop to take advantage of an adaptive finite element code such as KASKADE [1, 7, 8, 15]. The method is reliable and robust if the finite element solutions are accurate enough. The necessary accuracy is given by simple

formulas. The numerical examples presented nicely reflect the design principles discussed.

However, there is one major drawback of the black box use of the finite element code. The energy of the wave equation cannot be conserved exactly. Therefore one should think about *simple* modifications of the finite element module which would strictly guarantee energy conservation, not only within the accuracy of the elliptic solver.

The diffraction example shows that adaptivity can pay off for the wave equation, however, it does so only in the “shadow regions.” In the 2D case the “lighted region” tends to spread out everywhere thus producing nearly uniform triangulations after some time. However, in 3D due to the strong Huygens’ principle [20, p. 131] “shadow regions” are created after that a sharp signal has passed by. This generates large areas where coarse triangulations are a benefit in efficiency. Note, that we presented the algorithm for any spatial dimension. We therefore believe that our algorithm will be of particular interest in the 3D case.

Acknowledgements. It is a pleasure for us to thank Peter Deuffhard and Olof Widlund for their support and continuing interest in our work. Olof Widlund generously helped us to improve the English of our manuscript.

References

1. R. Beck, B. Erdmann, R. Roitzsch. KASKADE 3.0, an object-oriented adaptive finite element code. Technical Report 95-4, Konrad-Zuse-Zentrum, Berlin, 1995. URL = <http://www.zib.de/ZIBbib/Publications>.
2. F. A. Bornemann. An adaptive multilevel approach to parabolic equations I. General theory and 1D-implementation. *IMPACT Comput. Sci. Engrg.*, **2**:279–317, 1990.
3. F. A. Bornemann. An adaptive multilevel approach to parabolic equations II. Variable order time discretization based on a multiplicative error correction. *IMPACT Comput. Sci. Engrg.*, **3**:93–122, 1991.
4. F. A. Bornemann. An adaptive multilevel approach to parabolic equations III. 2D error estimation and multilevel preconditioning. *IMPACT Comput. Sci. Engrg.*, **4**:1–45, 1992.
5. F. A. Bornemann, P. Deuffhard. The cascadic multigrid method for elliptic problems. *Numer. Math.*, **75**:135–152, 1996.
6. F. A. Bornemann, P. Deuffhard. Cascadic Multigrid Methods. In: R. Glowinski, J. Pèriaux, Z.-C. Shi, O. Widlund, editors, *Domain Decomposition Methods in Sciences and Engineering. Proceedings of the 8th International Conference on Domain Decomposition Methods*, Beijing, China, May 1995, pages 205–212. John Wiley & Sons, Chichester, New York, 1997.
7. F. A. Bornemann, B. Erdmann, R. Kornhuber. Adaptive multilevel methods in three space dimensions. *Inter. J. Numer. Meth. Engrg.*, **36**:3187–3202, 1993.
8. F. A. Bornemann, B. Erdmann, R. Kornhuber. A posteriori error estimates for elliptic problems in two and three space dimensions. *SIAM J. Numer. Anal.*, **33**:1188–1204, 1996.
9. F. A. Bornemann, R. Krause. Classical and Cascadic Multigrid — A Methodical Comparison. In: P. Bjørstad, M. Espedal, D. Keyes, editors, *Proceedings of the 9th International Conference on Domain Decomposition Methods 1996*, Ullensvang, Norway, 1996. John Wiley & Sons, Chichester, New York, to appear.
10. J. H. Bramble, J. E. Pasciak, J. Xu. Parallel multilevel preconditioners. *Math. Comp.*, **55**:1–22, 1990.
11. B. Brenner, V. Thomée. On rational approximations of semigroups. *SIAM J. Numer. Anal.*, **16**:683–694, 1979.
12. P. Deuffhard. Cascadic conjugate gradient methods for elliptic partial differential equations. Algorithm and numerical results. In D. Keyes, J. Xu, editors, *Proceedings of the 7th International Conference on Domain Decomposition Methods 1993*, pages 29–42. AMS, Providence, 1994.
13. P. Deuffhard, F. A. Bornemann. *Numerische Mathematik II. Integration gewöhnlicher Differentialgleichungen*. Walter de Gruyter, Berlin, New York, 1994.
14. P. Deuffhard, J. Lang, U. Nowak. Recent progress in dynamical process simulation. In H. Neunzert, editor, *Progress in Industrial Mathematics, Proc. 8th Conference of the European Consortium for Mathematics in Industry (ECMI 94)*, Kaiserslautern, Germany, pages 122–137. Wiley-Teubner, Chichester, Stuttgart, 1996.
15. P. Deuffhard, P. Leinen, H. Yserentant. Concepts of an adaptive hierarchical finite element code. *IMPACT Comput. Sci. Engrg.*, **1**:3–35, 1989.
16. N. Dunford, J. T. Schwartz. *Linear Operators Part I: General Theory*. John Wiley, New York, Chichester, 1957.
17. E. Hairer, S. P. Nørsett, G. Wanner. *Solving Ordinary Differential Equations I. Nonstiff Problems*. Springer-Verlag, Berlin, Heidelberg, New York, 2. edition, 1993.
18. E. Hairer, G. Wanner. *Solving Ordinary Differential Equations II. Stiff and Differential-Algebraic Problems*. Springer-Verlag, Berlin, Heidelberg, New York, 1991.
19. E. Hille, R. S. Phillips. *Functional Analysis and Semi-Groups*. Amer. Math. Soc., Providence, 1957.
20. F. John. *Partial Differential Equations*. Springer-Verlag, Berlin, Heidelberg, New York, 4th edition, 1991.
21. T. Kato. *Perturbation Theory for Linear Operators*. Springer-Verlag, Berlin, Heidelberg, New York, 2nd edition, 1984.
22. J. Lang. Adaptive FEM for reaction-diffusion equations. Preprint 96-28, Konrad-Zuse-Zentrum, Berlin, 1996. URL = <http://www.zib.de/ZIBbib/Publications>.
23. A. Pazy. *Semigroups of Linear Operators and Applications to Partial Differential Equations*. Springer-Verlag, Berlin, Heidelberg, New York, 1983.
24. W. Rudin. *Functional Analysis*. McGraw-Hill, New York, 2nd edition, 1991.
25. F. Schmidt. An adaptive approach to the numerical solution of Fresnel's wave equation. *IEEE J. of Lightwave Tech.*, **11**:1425–1435, 1993.
26. F. Schmidt, H.-P. Nolting. Adaptive multilevel beam propagation method. *IEEE Photonics Tech. Lett.*, **4**:1381–1383, 1992.
27. G. Wanner, E. Hairer, S. P. Nørsett. When I -stability implies A -stability. *BIT*, **18**:503, 1978.
28. M. Wulkow. Adaptive treatment of polyreactions in weighted sequence spaces. *IMPACT Comput. Sci. Engrg.*, **4**:152–193, 1992.